6. Turro, N. J. *Modern Molecular Photochemistry* 1–195 (University Science, California, 1991).
7. Beljonne, D. *et al.* Spatial extent of the singlet and triplet excitons in transition metal-containing poly-ynes. *J. Chem. Phys.* **105**, 3868–3877 (1996).
8. Wittmann, H. F., Friend, R. H., Khan, M. S. & Lewis, J. Optical spectroscopy of platinum and palladium containing poly-ynes. *J. Chem. Phys.* **101**, 2693–2698 (1994).
9. Wilson, J. S. *et al.* Triplet states in a series of Pt-containing ethynylenes. *J. Chem. Phys.* **113**, 7627–7634 (2000).
10. Chawdhury, N. *et al.* Evolution of lowest singlet and triplet excited states with number of thienyl rings in platinum poly-ynes. *J. Chem. Phys.* **110**, 4963–4970 (1999).
11. Chawdhury, N. *et al.* Synthesis and electronic structure of platinum-containing poly-ynes with aromatic and heteroaromatic rings. *Macromolecules* **31**, 722–727 (1998).
12. Romanovskii, Y. V. *et al.* Phosphorescence of π-conjugated oligomers and polymers. *Phys. Rev. Lett.* **84**, 1027–1030 (2000).
13. Hertel, D. *et al.* Phosphorescence in conjugated poly(para-phenylene)-derivatives. *Adv. Mater.* **13**, 65–70 (2001).
14. Beljonne, D., Shuai, Z., Friend, R. H. & Brédas, J. L. Theoretical investigation of the lowest singlet and triplet states in poly(paraphenylene vinylene) oligomers. *J. Chem. Phys.* **102**, 2042–2049 (1995).
15. Wilson, J. S. *et al.* The energy gap law for triplet states in Pt-containing conjugated polymers and monomers. *J. Am. Chem. Soc.* **123**, 9412–9417 (2001).
16. Becker, H., Burns, S. E. & Friend, R. H. Effect of metal films on the photoluminescence and electroluminescence of conjugated polymers. *Phys. Rev. B* **56**, 1893–1905 (1997).
17. Kim, J. S., Ho, P. K. H., Greenham, N. C. & Friend, R. H. Electroluminescence emission pattern of organic light-emitting diodes: Implications for device efficiency calculations. *J. Appl. Phys.* **88**, 1073–1081 (2000).
18. Kobrak, M. N. & Bittner, E. R. Quantum molecular dynamics study of polaron recombination in conjugated polymers. *Phys. Rev. B* **62**, 11473–11486 (2000).
19. Blom, P. W., de Jong, M. J. M. & Breedijk, S. Temperature dependent electron-hole recombination in polymer light emitting diodes. *Appl. Phys. Lett.* **71**, 930–932 (1997).
20. Pope, M. & Swenberg, C. E. *Electronic Processes in Organic Crystals and Polymers* 2nd edn, 958–960 (Oxford Science, Oxford, 1999).
21. Shuai, Z., Beljonne, D., Silbey, R. J. & Brédas, J. L. Singlet and triplet exciton formation rates in conjugated polymer light-emitting diodes. *Phys. Rev. Lett.* **84**, 131–134 (2000).
22. Hong, T. & Meng, H. Spin-dependent recombination and electroluminescence quantum yield in conjugated polymers. *Phys. Rev. B* **63**, 1–5 (2001).
23. Burin, A. L. & Ratner, M. A. Spin effects on the luminescence yield of organic light emitting diodes. *J. Chem. Phys.* **109**, 6092–6102 (1998).

Superconductivity in single crystals of the fullerene C_{70}

J. H. Schön*†, Ch. Kloc*, T. Siegrist*‡, M. Steigerwald‡, C. Svensson§ & B. Batlogg*‖

* *Bell Laboratories, Lucent Technologies, 600 Mountain Avenue, Murray Hill, New Jersey 07974, USA*
† *Department of Physics, University of Konstanz, D-78457 Konstanz, Germany*
‡ *Agere Systems, 600 Mountain Avenue, Murray Hill, New Jersey 07974, USA*
§ *Inorganic Chemistry 2, PO Box 124, Lund University, S-221 00 Lund, Sweden*
‖ *Solid State Physics Laboratory ETH, CH-8093 Zürich, Switzerland*

The observation of superconductivity in doped C_{60} has attracted much attention[1–3], as these materials represent an entirely new class of superconductors. A maximum transition temperature (T_c) of 40 K has been reported[4] for electron-doped C_{60} crystals, while a T_c of 52 K has been seen[5] in hole-doped crystals; only the copper oxide superconductors have higher transition temperatures. The results for C_{60} raise the intriguing questions of whether conventional electron–phonon coupling alone[1] can produce such high transition temperatures, and whether even higher transition temperatures might be observed in other fullerenes[6–8]. There have, however, been no confirmed reports of superconductivity in other fullerenes, though it has recently been observed in carbon nanotubes[9]. Here we report the observation of superconductivity in single crystals of electric-field-doped C_{70}. The maximum transition temperature of about 7 K is achieved when the sample is doped to approximately four electrons per C_{70} molecule, which corresponds to a half-filled conduction band. We anticipate superconductivity in smaller fullerenes at temperatures even higher than in C_{60} if the right charge density can be induced.

Metallic behaviour is expected for KC_{70} and K_4C_{70} owing to the half-filling of the lowest unoccupied molecular orbital bands in K-intercalated C_{70}. An initial transport study on K-intercalated C_{70} found a maximum conductivity of $\sim 2\,S\,cm^{-1}$ (ref. 10). Theory and experiment showed that K_4C_{70} exhibits a larger conductivity because of its higher density of states[11–13]. Pure C_{70} and alkali-metal-doped C_{70} show non-zero resistance down to 1.8 K. The absence of superconductivity in these experiments is not well understood, and might be related to disorder and structural defects in the K_4C_{70} thin films. A weak electron–phonon interaction[11,14] and a reduced density of states at the Fermi level[15] have also been invoked as reasons for the apparent lack of superconductivity. We note, however, that most experiments have been performed on polycrystalline material, and phase-pure alkali-doped C_{70} analogues of A_3C_{60} have not been reported. In addition, various crystallographic structures of C_{70} have been observed[16]. Here we have chosen a different approach to induce electric charge in C_{70} crystals. We have recently demonstrated that the electrical properties of organic materials can be investigated over a wide range of charge density using field-effect doping, without inducing additional disorder[5,17–19], leading to gate-induced superconductivity in a variety of molecular organic crystals[5,17,18]. This method therefore seems to be well suited to our investigation of the reasons for the absence of superconductivity in the higher fullerenes—is it related to intrinsic properties, or to difficulties in chemical doping? Here we apply this technique to investigate the possibility of superconductivity in high-quality C_{70} single crystals.

We grew single crystals of C_{70} (smaller than 1 mm^3) from the vapour phase in a stream of hydrogen; the experimental conditions were similar to those used to grow C_{60} (ref. 5). The crystals were annealed in a xenon atmosphere, but we detected no incorporation of the inert gas into the crystals. We performed an X-ray structural analysis of the C_{70} single crystals, which showed them to be hexagonal closed packed (h.c.p.) C_{70}, with lattice parameters $a = 10.602(9)$ Å and $c = 17.263(13)$ Å. Previous studies of hexagonal C_{70} gave lattice parameters of $a = 10.104$ Å and $c = 18.584$ Å, with a wide mosaic spread of the order of a few degrees[20]—furthermore, these crystals showed diffuse rods typical of stacking faults[21]. In contrast, our crystals show a much narrower mosaic of the order of 0.4°. In addition, the c/a ratio for our crystals is close to the ideal value of 1.63 for sphere packing, in contrast to the reported value of 1.84. To first order, it is possible to approximate the ellipsoidal C_{70} molecule by a hollow sphere with radius $r = 3.78$ Å, and we obtained a residual of $R = 0.065$ for 118 independent reflections measured. As stacking faults were expected to be present, we looked for diffuse rods of intensity. Instead, we found well developed superstructure reflections with a mosaic spread of the order of 0.4° consistent with 6H polytypes, leading to a tripling of the c axis ($3c = 51.79$ Å). Different 6H stacking sequences are expected, producing twinning at room temperature. On average, five layers are stacked coherently, with the sixth in either the h.c.p. or the cubic close packed (c.c.p.) position. Low-temperature X-ray diffraction revealed a further lowering of symmetry, but the crystals clearly undergo multiple twinning upon cooling. This lowering of the symmetry is indicative of a transition to a phase in which the C_{70} molecules no longer rotate freely. However, we do not expect that the orientational order of the molecules will be complete, similar to the phase transition observed for C_{60} upon cooling[22]. Further structural studies at low temperature are under way.
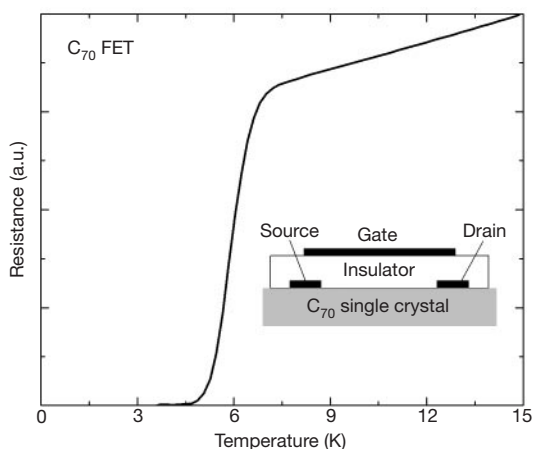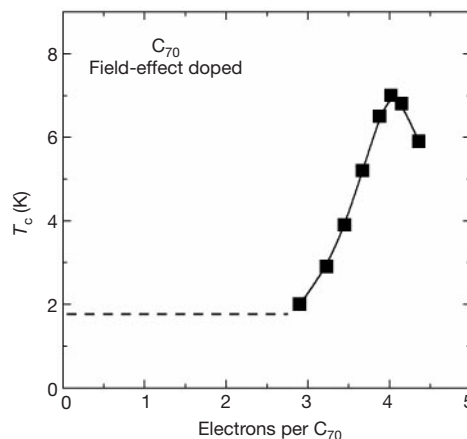
Figure 1 Resistance of a field-effect-doped C_{70} single crystal as a function of temperature. For a doping level of four electrons per molecule, a transition to superconductivity is observed, starting at ~7 K. Inset, diagram of the field-effect-device structure.

Figure 2 Transition temperature as a function of the doping level. A maximum T_c of 7 K is observed for four electrons per C_{70} molecule. The experimental doping range is limited by the breakdown of the gate insulator. The dashed line indicates the doping range where no superconductivity was observed above 1.7 K.

We prepared field-effect transistors (FETs) on growth surfaces by the deposition of source and drain electrodes made of gold, an Al_2O_3 gate insulator, and a gold gate electrode (see Fig. 1 inset). The transistors showed n-channel activity, with room-temperature mobilities in the range $1-1.8\ cm^2\ V^{-1}\ s^{-1}$. Similar mobilities have been reported for C_{60} single-crystal transistors[17]. We observed no p-channel activity, a fact that we ascribe to significantly stronger trapping of holes than of electrons. Such behaviour is often observed in organic FETs. We have studied the transport properties of C_{70} p-channel FETs down to 1.7 K in magnetic fields up to 9 T. The experimental field-effect-doping range is limited by the electrical breakdown of the gate insulator.

By applying a strong electric field to the gate, it is possible to induce a very high carrier concentration into the topmost layer of molecules in the organic crystal. Figure 1 shows the channel resistance as a function of temperature for a C_{70} FET. The electron density is approximately four electrons per C_{70} molecule, assuming that only the topmost layer takes part in the conduction[5,17–19]. The resistance starts to drop at 7 K, reaches its half-point at 6 K, and indicates a transition to the superconducting state. An external magnetic field, applied perpendicular to the FET channel, suppresses the transition as in C_{60} crystals[5,17]. From the estimated zero-temperature upper critical field, we calculate a coherence length of 40 Å for C_{70}, which is similar to values obtained for bulk-doped as well as field-effect-doped C_{60} (refs 2, 3, 17). The dependence of the transition temperature on the electron density is shown in Fig. 2. Superconductivity (above 1.7 K) is observed for more than three electrons per molecule. A maximum transition temperature of 7 K is observed for four electrons per C_{70} molecule. This density corresponds to half-filling of the conduction band[12]. We note that the highest conductivity of alkali-metal-doped C_{70} films has also been observed for this doping level[20]. However, band structure calculations[24] and photoemission data[25] have been interpreted as suggesting that the conduction band of C_{70} might take only six electrons. This would then raise the question of why superconductivity in C_{60} occurs around half-filling, and in C_{70} around two-thirds filling. Differences might arise from the cubic and hexagonal crystal structure of C_{60} and C_{70}, respectively. Further detailed theoretical and experimental studies into the electronic structure of C_{70} seem to be appropriate.

It is interesting to compare the transition temperatures of field-effect-doped C_{60} and C_{70}. In the larger molecule T_c is ~7 K, whereas it is ~11 K in the smaller one. This reduction is in line with the theoretical expectations of a reduced intra-molecule electron–phonon coupling strength[6]. But other effects also need to be considered—in particular, the electronic density of states and the effective Coulomb interaction strength.

Reports of superconductivity in members of the fullerene family other than C_{60} have not so far been confirmed[23]. The present results now indicate the strong possibility that other fullerenes might also become superconducting. This would be another way towards superconductivity at much higher temperatures: the electron–phonon coupling has been calculated to become stronger with decreasing numbers of π-electrons[6] and with increasing curvature of the molecules[26,27]. Thus it will be interesting to study the smaller fullerenes[7,8], and field-effect doping would seem to be the method of choice to introduce holes and electrons. The present results seem also to indicate the importance of reducing disorder in the crystals or in films. □

1. Hebard, A. F. et al. Superconductivity at 18 K in potassium-doped C_{60}. Nature **350**, 600–601 (1991).
2. Ramirez, A. P. C_{60} and its superconductivity. Supercond. Rev. **1**, 1–101 (1994).
3. Gunnarsson, O. Superconductivity in fullerides. Rev. Mod. Phys. **69**, 575–606 (1997).
4. Palstra, T. T. M. et al. Superconductivity at 40 K in cesium doped C_{60}. Solid State Commun. **93**, 327–330 (1995).
5. Schön, J. H., Kloc, Ch. & Batlogg, B. Superconductivity at 52 K in hole-doped C_{60}. Nature **408**, 549–552 (2000).
6. Devos, A. & Lannoo, M. Electron-phonon coupling for aromatic molecular crystals: Possible consequences for their superconductivity. Phys. Rev. B **58**, 8236–8239 (1998).
7. Cohen, M. L. Possibility of high temperature superconductivity in C_{36} and $C_{24}N_{12}$ solids. Am. Inst. Phys. Conf. Proc. **483**, 359–365 (1999).
8. Piskoti, C., Yarger, J. & Zettl, A. C_{36}, a new carbon solid. Nature **393**, 771–774 (1998).
9. Tang, Z. K. et al. Superconductivity in 4 Å single-walled carbon nanotubes. Science **292**, 2462–2465 (2001).
10. Haddon, R. C. et al. Conducting films of C_{60} and C_{70} by alkali-metal doping. Nature **350**, 320–322 (1991).
11. Wang, Z. H., Dresselhaus, M. S., Dresselhaus, G. & Eklund, P. C. Raman studies of electron-phonon interaction in K_xC_{70}. Phys. Rev. B **48**, 16881–16884 (1994).
12. Saito, S. & Oshiyama, A. Electronic and geometric structures of C_{70}. Phys. Rev. B **44**, 11532–11535 (1991).
13. Wang, Z. H. et al. Electronic properties of K_xC_{70} thin films. Phys. Rev. B **48**, 10657–10660 (1994).
14. Wang, Z. H., Dresselhaus, M. S., Dresselhaus, G., Wang, K. A. & Eklund, P. C. Electronic properties of K_xC_{70} thin films. II. Phys. Rev. B **49**, 15890–15900 (1994).
15. Takahashi, T. et al. Comparative photoemission study of Rb_xC_{60}, Rb_xC_{70} and RbC_8. A pseudo-gap at the Fermi level in the fulleride. Physica C **190**, 205–209 (1992).
16. Chen, X. H. et al. Synthesis, structure, and transport properties of novel fullerides A_3C_{70} (A = Ba and Sm). J. Am. Chem. Soc. **122**, 5729–5732 (2000).
17. Schön, J. H., Kloc, Ch., Haddon, R. C. & Batlogg, B. A superconducting field-effect switch. Science **288**, 656–658 (2000).
18. Schön, J. H., Kloc, Ch. & Batlogg, B. Superconductivity in molecular crystals induced by charge injection. Nature **406**, 704–706 (2000).

19. Schön, J. H. et al. Gate-induced superconductivity in solution-processed, organic polymer films. *Nature* **410**, 189–192 (2001).
20. Blanc, H.-B. et al. Single-crystal X-ray diffraction study of the room temperature structure and orientational disorder of C$_{70}$. *Europhys. Lett.* **27**, 359–364 (1994).
21. Blanc, E., Bürgi, H.-B., Restori, R., Schwarzenbach, D. & Ochsenbein, Ph. X-ray diffraction study of the stacking faults in hexagonal C$_{70}$ single crystals. *Europhys. Lett.* **33**, 205–210 (1996)
22. Bürgi, H. B. et al. The structure of C$_{60}$: orientational disorder in the low-temperature modification of C$_{60}$. *Angew. Chem. Int. Edn Engl.* **31**, 640–643 (1992).
23. Wang, Z. H. et al. Electronic properties of K$_x$C$_{70}$ thin films. *Phys. Rev. B* **48**, 10657–10660 (1994).
24. Ohno, K., Jing-Zhi, Y., Maruyama, Y., Kawazoe, Y. & Takahashi, T. Electronic structures of C$_{70}$ crystalline phases. *Chem. Phys. Lett.* **255**, 367–372 (1996).
25. Golden, M. S. et al. The electronic structure of fullerenes and fullerene compounds from high-energy spectroscopy. *J. Phys. Condens. Matter* **7**, 8219–8247 (1995).
26. Kobayashi, M. et al. Structure sequence and possible superconductivity in potassium-doped fullerene C$_{70}$K$_x$. *Phys. Rev. B* **48**, 16877–16880 (1993).
27. Schluter, M., Lannoo, M., Needles, M. & Baraff, G. A. Electron-phonon coupling and super-conductivity in alkali-intercalated C$_{60}$ solid. *Phys. Rev. Lett.* **68**, 526–529 (1992).

....

Magma storage beneath Axial volcano on the Juan de Fuca mid-ocean ridge

M. West*†, **W. Menke***†, **M. Tolstoy***, **S. Webb***† & **R. Sohn**‡

* *Lamont-Doherty Earth Observatory of Columbia University, Palisades, New York 10964, USA*
† *Department of Earth and Environmental Science, Columbia University, Palisades, New York 10964, USA*
‡ *Woods Hole Oceanographic Institution, Woods Hole, Massachusetts 02543, USA*

....

Axial volcano, which is located near the intersection of the Juan de Fuca ridge and the Cobb–Eickelberg seamount chain beneath the northeast Pacific Ocean, is a locus of volcanic activity thought to be associated with the Cobb hotspot[1]. The volcano rises 700 metres above the ridge, has substantial rift zones extending about 50 kilometres to the north and south, and has erupted as recently as 1998 (ref. 2). Here we present seismological data that constrain the three-dimensional velocity structure beneath the volcano. We image a large low-velocity zone in the crust, consisting of a shallow magma chamber and a more diffuse reservoir in the lower crust, and estimate the total magma volume in the system to be between 5 and 21 km^3. This volume is two orders of magnitude larger than the amount of melt emplaced during the most recent eruption[3,4] (0.1–0.2 km^3). We therefore infer that such volcanic events remove only a small portion of the reservoir that they tap, which must accordingly be long-lived compared to the eruption cycle. On the basis of magma flux estimates, we estimate the crustal residence time of melt in the volcanic system to be a few hundred to a few thousand years.

Axial volcano is formed by excess magmatism associated with mantle melting at the Cobb hotspot and the Juan de Fuca ridge[5]. Shoaling bathymetry, inferred crustal thickening[6], frequent seismic swarms[7,8] and deformation events[3,4] are consistent with a robust magma supply system. Lateral dyke injection, observed during a 1998 eruption[9], originated from a source under the caldera and carried magma up to 50 km along the volcano's rift zones, which are substantial constructional features. Such events suggest that magma supply is strongly focused beneath the volcano. The existence of the 3 × 8 km caldera, its 3 m subsidence during the 1998 eruption[10], and evidence for low-density rock beneath the summit[11], suggest a large

magma body a few kilometres beneath the volcano. What has not been understood is how much melt exists, how long it spends in the crust, and how eruptions along the rifts and adjacent ridge segments are related to the magma reservoir. These questions have remained unanswered, not just at Axial volcano, but at basaltic shield volcanoes worldwide.

The compressional-velocity image of the volcano presented here is based on data collected during a 1999 active-source seismic experiment (Fig. 1). 5,025 shots from the airgun array (20 guns totalling 142 litres) of the RV *Maurice Ewing* were recorded on six ocean-bottom seismometers[12] deployed on the volcano's flanks. Water wave travel times and global positioning system (GPS)-determined shot locations were used to precisely locate the seismometers on the sea floor (error < 20 m) and to determine clock drifts (error < 0.02 s). Travel times from 16,400 Pg phases, which turn within the crust, are used in this study.

To characterize the regional structure, a bathymetry-draped one-dimensional (1D) velocity model was assembled from previous studies[13,14] on the Juan de Fuca ridge. Predicted travel-time errors through this model were inverted to determine the best-fit 1D velocity structure (see Methods). Seismic ray-paths crossing the caldera were excluded from the inversion, so the resulting model represents average crustal structure away from the volcano. In the final 1D model (not shown), velocity contours 4–6 km s^{-1} are up to 1 km deeper than on other parts of the Juan de Fuca[13,14] ridge. The additional 0.5–1.0 km of volcanic extrusives implied by these depressed velocities is not surprising, considering the shallow bathymetry and crustal thickening[6].

Seismic travel-time prediction was accomplished through a fast ray shooting method performed on a three-dimensional tetrahedral velocity grid. Predicted travel times through the 1D model deviate from real data with an r.m.s. error of 0.181 s. Much of this misfit is contributed by a small number of caldera-crossing rays which are systematically delayed by up to 0.5 s (Fig. 2). A three-dimensional
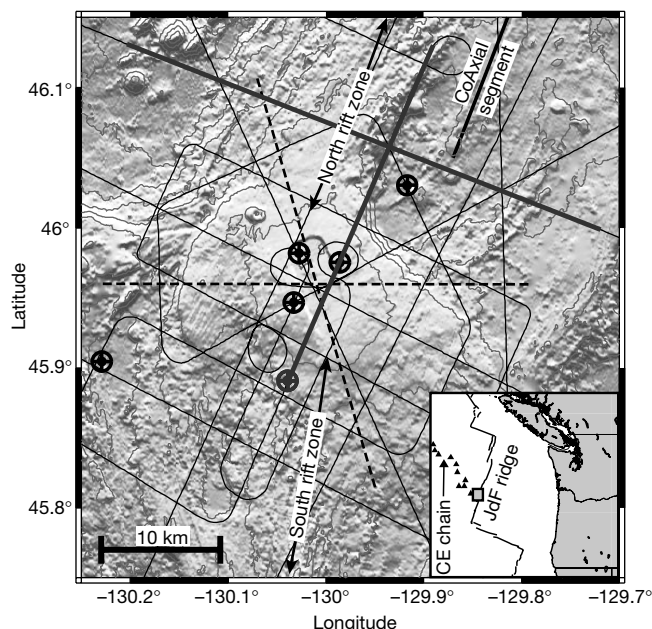
Figure 1 Bathymetry of Axial volcano. Summit caldera, in centre of figure, is at ~1,460 m depth, surrounding sea floor is at ~2,800 m depth, contour interval is 200 m. Thin black lines mark airgun shot lines, crossed circles with central dot show ocean-bottom seismometers used in analysis. Two dashed lines mark cross-sections in Fig. 4. The two crossing thick black lines, one of which ends in a seismometer, display source–receiver geometry for Fig. 2. Scale bar, 10 km. Inset, location of experiment on the Juan de Fuca (JdF) ridge, and the seamounts in the Cobb–Eickelberg (CE) chain.

833

letters to nature

25. Reck-Peterson, S. L., Novick, P. J. & Mooseker, M. S. The tail of a yeast class V myosin, myo2p, functions as a localization domain. *Mol. Biol. Cell* **10**, 1001–1017 (1999).

26. Gomes de Mesquita, D. S., van den Hazel, H. B., Bouwman, J. & Woldringh, C. L. Characterization of new vacuolar segregation mutants, isolated by screening for loss of proteinase B self-activation. *Eur. J. Cell Biol.* **71**, 237–247 (1996).

27. Hill, K. L., Catlett, N. L. & Weisman, L. S. Actin and myosin function in directed vacuole movement during cell division in *Saccharomyces cerevisiae*. *J. Cell Biol.* **135**, 1535–1549 (1996).

28. Catlett, N. L. & Weisman, L. S. The terminal tail region of a yeast myosin-V mediates its attachment to vacuole membranes and sites of polarized growth. *Proc. Natl Acad. Sci. USA* **95**, 14799–14804 (1998).

29. Catlett, N. L. & Weisman, L. S. Divide and multiply: organelle partitioning in yeast. *Curr. Opin. Cell Biol.* **12**, 509–516 (2000).

....

retractions

Superconductivity in CaCuO₂ as a result of field-effect doping

J. H. Schön, M. Dorget, F. C. Beuran, X. Z. Zu, E. Arushanov, C. Deville Cavellin & M. Laguës

Nature **414**, 434–436 (2001).

This manuscript was, in part, the subject of an independent investigation[1] conducted at the behest of Bell Laboratories, Lucent Technologies. The independent committee reviewed concerns related to the validity of data associated with the device measurements described in the paper.

J.H.S.: As a result of the committee's findings[1], I am issuing a retraction of the paper. I note nevertheless that this paper may also contain some legitimate ideas and contributions.

M.D., X.Z.Z., E.A. and C.D.C.: In the light of the recent findings of the investigation[1] committee chaired by Professor Beasley, we would like to warn readers about the validity of the field-effect doping data presented in this paper and issue a retraction of this article. Our laboratory specializes in the synthesis, by molecular beam epitaxy, of copper oxide thin films. In May 2001, we initiated a collaboration with J.H.S., in which our role was limited to the synthesis of a thin-film sample of CaCuO₂. We can certify the quality (composition and structure) of the sample, and we are ready to prepare such samples for other serious scientific teams who want to try to reproduce these results.

M.L. and F.C.B.: We comment here as researchers at Wintici SA, a technology company. The synthesis of the CaCuO₂ sample reported in the paper was undertaken in collaboration with researchers from ESPCI, and we can vouch for its quality. But in the light of the committee's findings[1], we wish to issue a retraction of the paper. We note nevertheless that this paper may also contain some legitimate ideas and contributions. □

1. Beasley, M. R., Datta, S., Kogelnik, H., Kroemer, H. & Monroe, D. Report of the Investigation Committee on the Possibility of Scientific Misconduct in the Work of Hendrik Schön and Coauthors. ⟨http://publish.aps.org/reports/⟩ (doi:10.1103/aps.reports.lucent) (Lucent Technologies/American Physical Society, September 2002).

Superconductivity in single crystals of the fullerene C₇₀

J. H. Schön, Ch. Kloc, T. Siegrist, M. Steigerwald, C. Svensson & B. Batlogg

Nature **413**, 831–833 (2001).

This manuscript was, in part, the subject of an independent investigation[1] conducted at the behest of Bell Laboratories, Lucent Technologies. The independent committee reviewed concerns related to the validity of data associated with the device measurements described in the paper. As a result of the committee's findings, we are issuing a retraction of the paper. We note nevertheless that this paper may also contain some legitimate ideas and contributions. □

1. Beasley, M. R., Datta, S., Kogelnik, H., Kroemer, H. & Monroe, D. Report of the Investigation Committee on the Possibility of Scientific Misconduct in the Work of Hendrik Schön and Coauthors. ⟨http://publish.aps.org/reports/⟩ (doi:10.1103/aps.reports.lucent) (Lucent Technologies/American Physical Society, September 2002).

Self-assembled monolayer organic field-effect transistors

Jan Hendrik Schön, Hong Meng & Zhenan Bao

Nature **413**, 713–716 (2001); correction *Nature* **414**, 470 (2001).

This manuscript was, in part, the subject of an independent investigation[1] conducted at the behest of Bell Laboratories, Lucent Technologies. The independent committee reviewed concerns related to the validity of data associated with the device measurements described in the paper. As a result of the committee's findings, we are issuing a retraction of the paper. We note nevertheless that this paper may also contain some legitimate ideas and contributions. □

1. Beasley, M. R., Datta, S., Kogelnik, H., Kroemer, H. & Monroe, D. Report of the Investigation Committee on the Possibility of Scientific Misconduct in the Work of Hendrik Schön and Coauthors. ⟨http://publish.aps.org/reports/⟩ (doi:10.1103/aps.reports.lucent) (Lucent Technologies/American Physical Society, September 2002).

Gate-induced superconductivity in a solution-processed organic polymer film

J. H. Schön, A. Dodabalapur, Z. Bao, Ch. Kloc, O. Schenker & B. Batlogg

Nature **410**, 189–192 (2001).

This manuscript was, in part, the subject of an independent investigation[1] conducted at the behest of Bell Laboratories, Lucent Technologies. The independent committee reviewed concerns related to the validity of data associated with the device measurements described in the paper. As a result of the committee's findings, we are issuing a retraction of the paper. We note nevertheless that this paper may also contain some legitimate ideas and contributions. □

1. Beasley, M. R., Datta, S., Kogelnik, H., Kroemer, H. & Monroe, D. Report of the Investigation Committee on the Possibility of Scientific Misconduct in the Work of Hendrik Schön and Coauthors. ⟨http://publish.aps.org/reports/⟩ (doi:10.1103/aps.reports.lucent) (Lucent Technologies/American Physical Society, September 2002).